Desalination and Water Treatment
www.deswater.com
doi: 10.5004/dwt.2023.29599

295 (2023) 245–254
May

Modified Tunisian diatomite for the removal of dyes: kinetic and thermodynamic studies

Houwaida Nefzi[a,b], Nadia Tahari[a,b], Olfa Bachrouch[a], Manef Abderrabbaa[a], Jalel Labidi[b,*]

[a]*Laboratory of Materials, Molecules and Applications, IPEST, Preparatory Institute of Scientific and Technical Studies of Tunis, University of Carthage, Sidi Bou Said Road, B.P.512070, La Marsa, Tunisia, emails: houayda.89@gmail.com (H. Nefzi), abderrabbamanef@gmail.com (M. Abderrabba), Olfabachrouch18@gmail.com (O. Bachrouch)*
[b]*Biorefinery Processes Research Group, Department of Chemical and Environmental Engineering, University of the Basque Country (UPV/EHU), Plaza, Europa 1, 20018 Donostia-San Sebastian, Spain, email: Jalel.Labidi@ehu.es*

Received 24 November 2022; Accepted 22 April 2023

ABSTRACT

Natural Tunisian diatomite powder (ND) and diatomite modified by activated carbon and beads (DAA) were synthesized for the elimination of two dyes Methylene blue (MB) and Congo red (CR). The different parameters effects on the adsorption process, like solution pH, temperature and initial concentration were studied. Our results confirmed that the percentage removal on the ND was detected to be 73.15% (19.95 mg/g) and 72.63% (44.93 mg/g) for MB and CR, respectively. However, this percentage was increased after combination with alginate and activated carbon to 96.72% (30.02 mg/g) for MB and 97.21% (85.32 mg/g) for CR. In addition, the adsorption kinetics followed the pseudo-second-order model, and the adsorption of dyes can be described by the Freundlich isotherm. Thus, our study affirmed the important role of DAA composite for the removal of cationic and anionic dye.

Keywords: Adsorption; Tunisian diatomite; Activated carbon; Alginate; Dyes

1. Introduction

The pollution of water represents a major problem for the environment and humans. Water can be polluted in different ways. One of the most polluting being wastewater from industries. Which contains various toxic compounds (dyes, heavy metals, etc.) [1]. Among these compounds, 7,105 tons of dyes produced annually, and a small quantity was released by allied industries or textile [2]. Despite the important increase of the use of dyes, the real quantity employed can vary 50% of the reactive used dyes can be lost [3,4].

Dyes are composed of different groups of atoms such as anthraquinone, carbonyl group or metinic group and their classification is based on their chemical structure [5]. In addition, they are very resistant to aerobic digestion for thus, they can resist heat, oxidizing agents, and light agents [6]. Cationic and anionic dyes are used in various domain, paper food, textiles, pharmaceuticals, etc. However, some of them have a dangerous effect on human health and environment because of their carcinogenic properties. In general, the effluents from various industries contain colorants, which can stay for a big time in water.

Methylene blue (MB), for example, is a cationic dye soluble in water and very used for medicinal purposes, wood and dying cotton [7]. However, it can cause nausea heart rate increasing, vomiting and skin or eye irritation [8]. Among anionic dyes, Congo red (CR) which is very used in many industries [9]. It is very resistant to biodegradation because of its structural stability [10]. However, it is a very harmful dye and toxic to many organisms [11]. For thus, it is considered a carcinogen and mutagen dye. Therefore, it is very necessary to eliminate these dyes from water using an easy and efficient technique.

* Corresponding author.

Various techniques of the elimination of dyes from water have been applied such as coagulation [12], aerobic or anaerobic digestion [13,14] and adsorption [15,16]. Among these methods, adsorption is the most simple, efficient, and rapid technique [17,18]. The most used adsorbent is activated carbon due to its high specific surface area and surface reactivity [19]. However, this adsorbent has many drawbacks such as the costs. Thus, this drawback can be reduced using a natural adsorbent.

Diatomaceous earth (DE) is a pale sedimentary rock. It has a specifics characteristic such as a porous structure, high permeability (80%–90% pore space), low conductivity coefficient, low-density, small particle size (10–200 μM) and large surface area [20,21]. It consists of an important quantity of SiO_2 and low quantities of minerals components (Al_2O_3, Fe_2O_3, etc.) [22]. In addition, the reactivity of DE is associated essentially with the reactivity of the acid sites on the surface of the amorphous silica and of the hydroxyl groups [23]. Recently, various research focused on the use of natural and modified DE as an adsorbent for the removal of dyes [24–26].

Alginates are produced from brown algae; they are a natural polysaccharide. They are low-cost products because of their easy extraction process and also their bioavailability [27]. Due to their versatile properties, alginates are very employed in different applications. In other hand, the viscosity of aqueous solution needs the use of alginates [28]. They are also apt to yield hydrogel in the presence of cations. Furthermore, the application of calcium alginate can be in immobilizing activated carbon [29], carbon nanotubes [30], magnetite nanoparticles [31] to produce good adsorbents to eliminate organic or inorganic pollutants from water [32].

Therefore, the objectives of this research were firstly the preparation of new natural adsorbent from the combination of diatomite-alginate and activated carbon beads (DAA) using simple preparation method. Secondly, to compare the adsorption capacity of natural diatomite powder and modified diatomite beads for the removal of MB and CR from aqueous solution. Afterwards, several characterization methods, such as scanning electron microscopy (SEM), Fourier-transform infrared spectroscopy (FTIR) and X-ray diffraction (XRD) were performed to determine the physical and chemical properties of the diatomite before and after surface modification. The dyes Methylene blue (MB) and Congo red, representing cationic dyes and anionic dyes, respectively, were selected as two target pollutants to analyze the process. In addition, adsorption parameters including initial concentration and pH were also monitored and discussed to investigate the effect of modification. Moreover, for a well-rounded and systematic evaluation, the adsorption kinetic and isotherm of various dye molecules were also discussed. The thermodynamic study was also discussed.

2. Materials and methods

2.1. Chemicals

The raw diatomite sample was obtained from Metlaoui (Gafsa, Tunisia). DE has been treated using chlorohydric acid (HCl) (PanReac, Castellar del Vallès, Spain, ACS Reagent, 37%), sodium hydroxide (NaOH) (PanReac, Castellar del Vallès, Spain, 98%), sodium chloride (NaCl) (PanReac, Castellar del Vallès, Spain, 98%), sodium alginate (Sigma-Aldrich, USA ≥98%), calcium chloride $CaCl_2$ (Sigma-Aldrich, USA ≥93%), activated carbon (Sigma-Aldrich, USA) were used to prepare the beads of modified diatomite. The chemical tested were Methylene blue and Congo red (Merck, Darmstadt, Germany). All the chemical components were used directly in the laboratory with any purification.

2.2. Preparation of diatomite

In order to obtain a powder of diatomite, the raw sample was completely crushed with hammers. The purification was carried out using a chlorohydric acid solution HCl (2 M) to eliminate impurities such us calcite. Thus, diatomite was added in the acid at a 10% ratio of solid (g)/liquid (mL), for 3 h at room temperature. Then, the sample was rinsed with distilled water and HCl for a several of times. Finally, it was dried in a vacuum oven at 100°C for 1 d.

2.3. Preparation of modified diatomite beads

The beads of diatomite-activated carbon were prepared with an alginate sodium solution. For thus, 100 mL of distilled water was used to dissolve sodium alginate (2 g) while stirring for 1 h. Then, an equal quantity of purified diatomite (2 g) and activated carbon (2 g) were mixed and added. Then, a 4% (w/v) of calcium chloride was used for the preparation of beads form. Finally, the beads were washed various times with distilled water. Thus, the proposed mechanism of the adsorption of MB and CR on the prepared beads is illustrated in Fig. 1.

2.4. Characterization of the material

In order to determine the point of zero charge pH_{pzc} of diatomite the same procedure of Son et al. has been used [33]. For thus, 40 mL of distilled water mixed with 5 mL of 0.1 M NaCl and were added in different flasks. Basic and acid solution NaOH (0.1 M) HCl (0.1 M) have been used to adjust the pH value (pH_i) (from 2 to 9). The final volume of solution in each flask was 50 mL. Then, we added 0.1 g of diatomite. After 24 h of stirring, we measured the final pH (pH_f). Thus, the ΔpH which is the difference between pH_i and pH_i was plotted against the pH_{pzc} was founded by the pH_i of intersection of curve with abscissa, at ΔpH = 0. In addition, the natural Tunisian diatomite powder (ND) was analyzed by powder XRD via a PANalytical CubiX^3 diffractometer using CuKα (λCuKα-media = 1.5418 Å, λCuKα1 = 1.54060 Å, λCuKα2 = 1.54439 Å) radiation (operating at 40 kV and 40 mA) over the angular range of 5°–70° 2θ (step size = 0.04 and time per step = 353 s) at room temperature.

In other hand, the X-ray fluorescence (XRF) technique was used to identify the composition of the prepared diatomite. Moreover, ND and DAA were characterized using FTIR technique (ATR-FTIR, PerkinElmer Spectrum, Madrid, Spain).

2.5. Batch adsorption study

The adsorption was studied by mixing 100 mg of beads with 100 mL of solution with various initial concentrations of dyes (10, 20 and 30 mg/L for MB, 20, 40 and

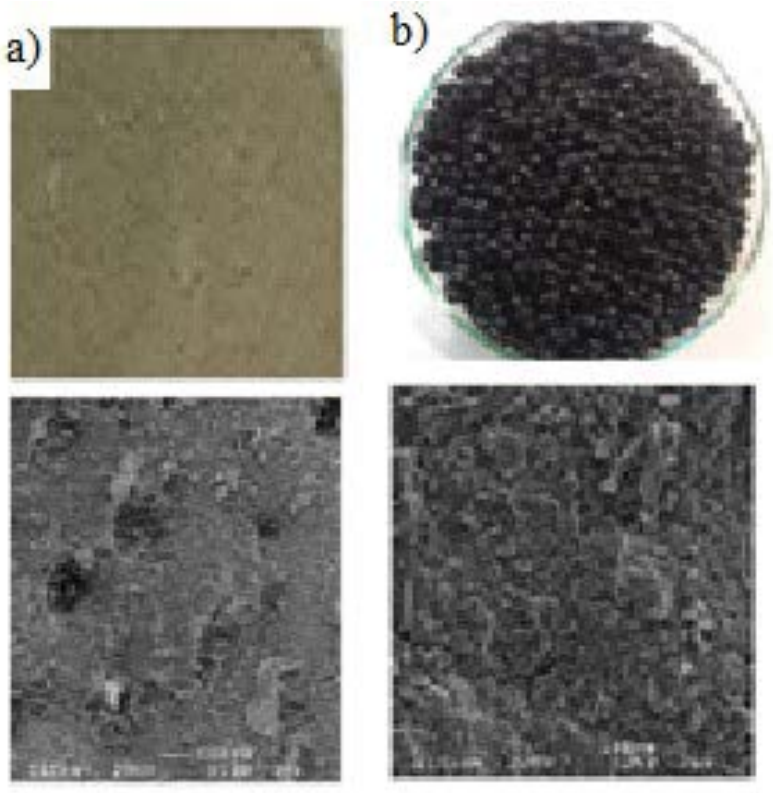

Fig. 1. Synthesis and mechanism of the adsorption of Methylene blue and Congo red on modified diatomite.

60 mg/L for CR). The mixture was kept under agitation at 150 rpm overnight to attain the equilibrium conditions. The absorbance change was determined at different time intervals. The comparison between the adsorption capacity of purified DE and DAA was studied. The mixture was filtered using a membrane filter. The analysis was immediately made by spectrophotometer (JASCO V-630, Tokyo, Japan) at the λ_{max} 670 nm for Methylene blue [34] and 497 nm for Congo red [35]. The quantity of adsorbed dyes (Q_t) (mg/g), at time t (min), obtained is as follows:

$$Q_{ads}=\left(C_o-C_t\right)\times\frac{V}{m} \quad (1)$$

where C_o and C_t are concentration (mg/g) at t = 0 and the concentration (mg/g) at time t, respectively, m is the mass of adsorbent and V is the volume of the solution.

3. Results

3.1. Surfaces properties of adsorbents

3.1.1. Scanning electron microscopy

The surface morphology of prepared beads and natural diatomite were evaluated using a SEM technique. Fig. 2a and b show purified diatomite and diatomite beads, respectively. The images indicate that Tunisian diatomite is rich in diatoms. It can be also observed that the tops of diatoms are often broken but their structures remain very well preserved. Furthermore, diatomite has a porous structure. Fig. 2b represents the used morphology for the preparation of the modified diatomite with sodium alginate and activated carbon.

3.1.2. X-ray fluorescence and X-ray diffraction

The quantitative analysis was achieved via XRF. The major constituent of raw diatomite was SiO_2 (29.60%) which explains that this rock is not pure. In addition, it contains various important elements (calcium, potassium, sodium, metals and alkaline earth metals, etc.). As shown in Table 1, the treatment with acid solution increased the amount of silica to 78.83%.

Fig. 3 shows the XRD analysis results of DE. The results showed the presence of three peaks at 31.96°, 26.66° and 21.75° confirmed that diatomite is rich with silica SiO_2 and other mineral components (Al_2O_3, Fe_2O_3, MgO, etc.).

3.1.3. Fourier-transform infrared spectroscopy

The analysis of ND and DAA by FTIR technique are presented in Fig. 4. In order to describe the surface characteristics of adsorbents, the analysis was determined between 450 and 4,000 cm^{-1}. We can distinguish from the spectrum 4a of a peak at 1,431 cm^{-1} in the spectrum of raw diatomite, and was completely disappeared after the treatment with acid solution. Fig. 4b confirms the presence of four specifics peaks at 3,395; 1,650; 1,023; 790 and 465 cm^{-1}. However, the specific peaks in the spectrum of modified diatomite are at 3,495; 3,000; 1,650 and 1,388 cm^{-1}.

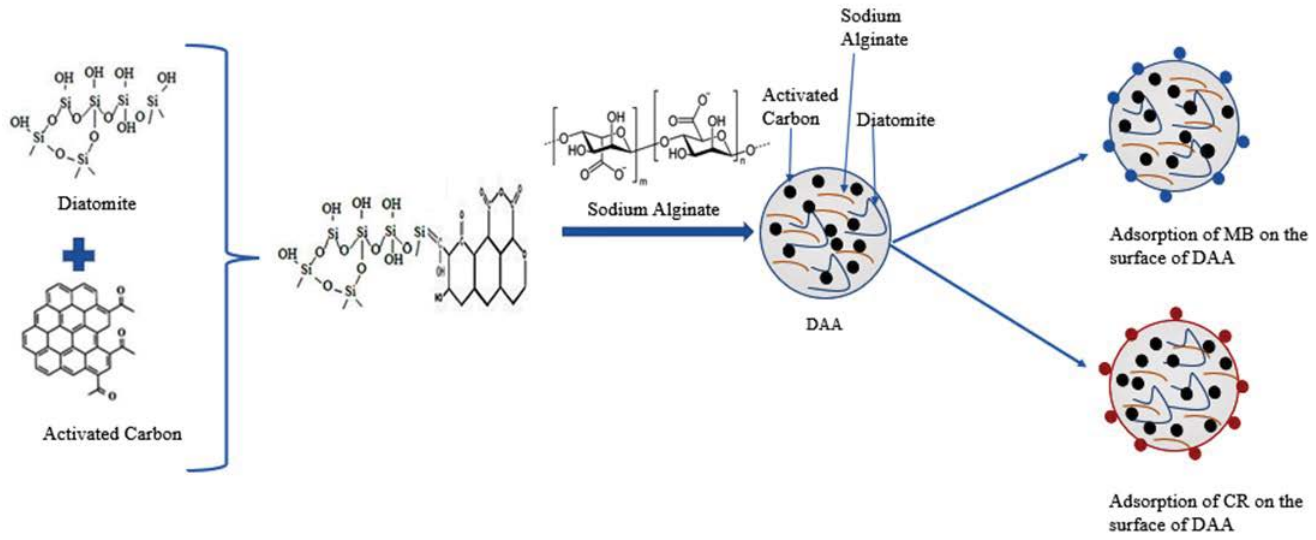

Fig. 2. Scanning electron microscopy of ND and DAA.

Table 1
Chemical composition of Tunisian diatomite before and after treatment

	Composition of diatomite before purification (%)	Composition of diatomite after purification (%)
SiO_2	29.0	78.83
Al_2O_3	2.57	6.53
Fe_2O_3	1.08	2.52
MnO	0.00	0.00
MgO	5.78	2.01
CaO	0.20	0.59
Na_2O	26.89	0.00
K_2O	0.39	0.96
TiO_2	0.16	0.38
P_2O_5	4.12	0.05
LOI	28.11	8.10

3.2. Effects operational parameter on MB and CR adsorption

3.2.1. Initial concentration effect

The evaluation of the effect of concentration on the adsorption process, the initial concentration differed from 10 to 30 mg/L for the MB and from 20 to 60 mg/L for the CR. The results show the remove of dyes increase with its initial concentration (Fig. 5). Thus, the initial concentration of dyes and a faster equilibrium was achieved at lower concentration. In addition, the first step of adsorption process was rapid (from 0 to 15 min for MB and from 0 to 10 min for CR).

3.2.2. Effect of pH

The evaluation of the influence of pH on the adsorption capacity is essentially related to the pH_{pzc} value of the adsorbent, which is 5.4. The adsorbent carries a positive charge at pH below 5.4 (Fig. 6). Thus, the impact of the solution pH (pH = 3–12) on MB and CR removal for ND and DAA is provided in Fig. 7. The results showed a sharp increase in the adsorption capacity of MB and CR at pH 6 and 3, respectively.

3.3. Adsorption kinetic model

The kinetic of dyes adsorption was determined with the two models (the pseudo-first and second-order model). Thus, the calculated kinetic parameters of the two models show that the correlation coefficient (R^2) is close to 1 (Table 2), Nevertheless, (R_1) of the pseudo-first-order is far from 1, as well, the calculated Q_e and experimental Q_e are not close.

$$\log\left(Q_e - Q_t\right) = -k_1 t + \log Q_e \text{ [36]} \tag{2}$$

$$\frac{t}{Q_t} = \frac{1}{k_2 \cdot Q_e^2} + \frac{1}{Q_e} \cdot t \text{ [37]} \tag{3}$$

where Q_t: quantity of dyes adsorption at different time, Q_e: quantity of dyes at equilibrium, k_1 (g/mg·min): constant of pseudo-first-order adsorption.

3.4. Adsorption isotherm

Dye adsorption isotherms have been described using Freundlich and Langmuir models [Eqs. (4) and (5), respectively]. The parameters of these two models are reported in Table 3. The results showed that the value of the regression coefficient R^2 Langmuir is superior that R^2 of Freundlich. In addition, the values of n given by the Freundlich model ($1/n < 1$).

$$\log Q_e = \log K_f + \frac{1}{n}\log C_e \text{ [38]} \tag{4}$$

where Q_e: adsorption quantity of dyes at equilibrium; C_e: concentration of dyes at equilibrium; K_f: constant of Freundlich.

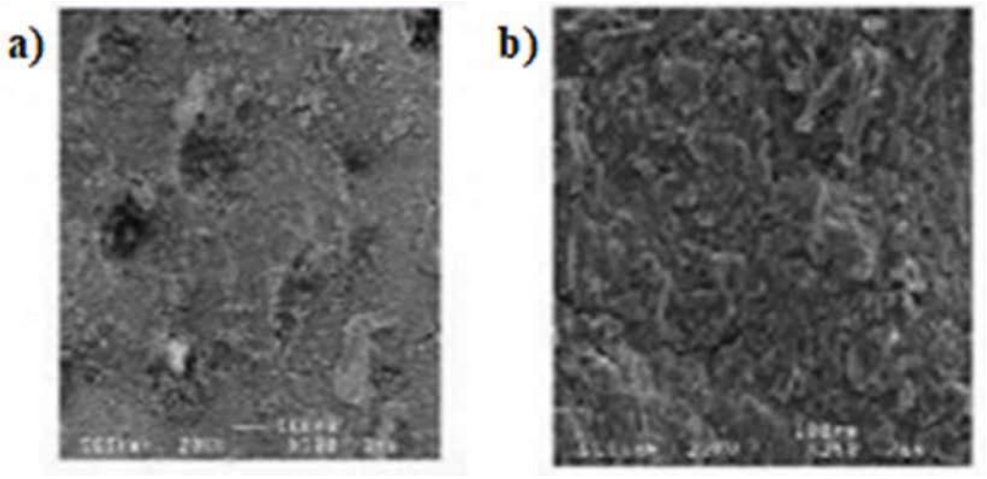

Fig. 3. X-ray diffraction of raw (a) and purified diatomite (b).

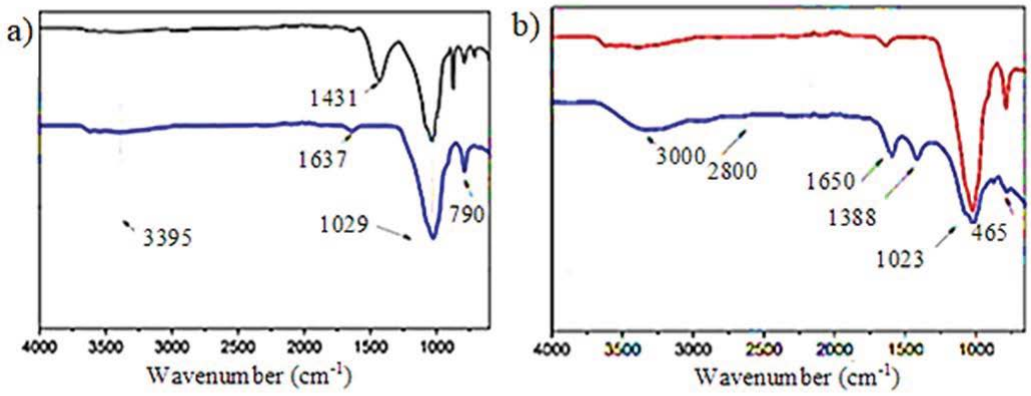

Fig. 4. Fourier-transform infrared spectroscopy of ND (a) and DAA (b).

$$\frac{C_e}{Q_e}=\left(\frac{1}{K_l\cdot Q_m}\right)+\left(\frac{C_e}{Q_m}\right)\text{[39]} \quad (5)$$

where Q_e: adsorption quantity of dyes at equilibrium; C_e: concentration at equilibrium; Q_m: constant of the occupied area by a monolayer of dyes (mg/g); K_l: constant of Langmuir.

3.5. Thermodynamic study

The values of the various parameters are shown in Table 4. Thus, $\Delta H°$ and $\Delta S°$ were determined by plotting the curve $\ln K_d = f(1/T)$. According to Table 4, the values of $\Delta H°$ and $\Delta S°$ are negative. In other hand, $\Delta G°$ values are positive for the adsorption of MB at 45°C.

4. Discussions

4.1. Surfaces properties of adsorbents

4.1.1. Scanning electron microscopy

The results confirm that the acid solution decreased the particle size of the natural materials, collapse and surface erosion. Then, the small particle size on the material is caused by the treatment with the acid solution. Similar results were obtained by Kır et al. [40] using Turkish diatomaceous earth. SEM analysis confirms that the beads contain numerous balls of all the composites which causes a heterogeneous and rough surface [41].

4.1.2. X-ray fluorescence and X-ray diffraction

Our results are the same reported by Ikusika et al. [42], thus they used diatomite from different sources which have an important quantity of SiO_2 (between 62.8% and 90.1%). The characteristics peaks of diatomite are 31.96°, 26.66° and 21.75°. Thus, the three types of silica (cristobalite, tridymite and quartz) were identified [43].

4.1.3. Fourier-transform infrared spectroscopy

The spectrum of raw diatomite confirms the presence of calcite at 1,431 cm^{-1}, the absence of this peak in the spectrum of treated diatomite confirms that the acid solution was efficient to eliminate impurities. In addition, the two absorption peaks 3,395; 1,650 and 3,395 cm^{-1} are attributed hydroxyl groups (O–H) [44]. In addition, around 1,023 and 465 cm^{-1} are two vibrations which can be attributed to the

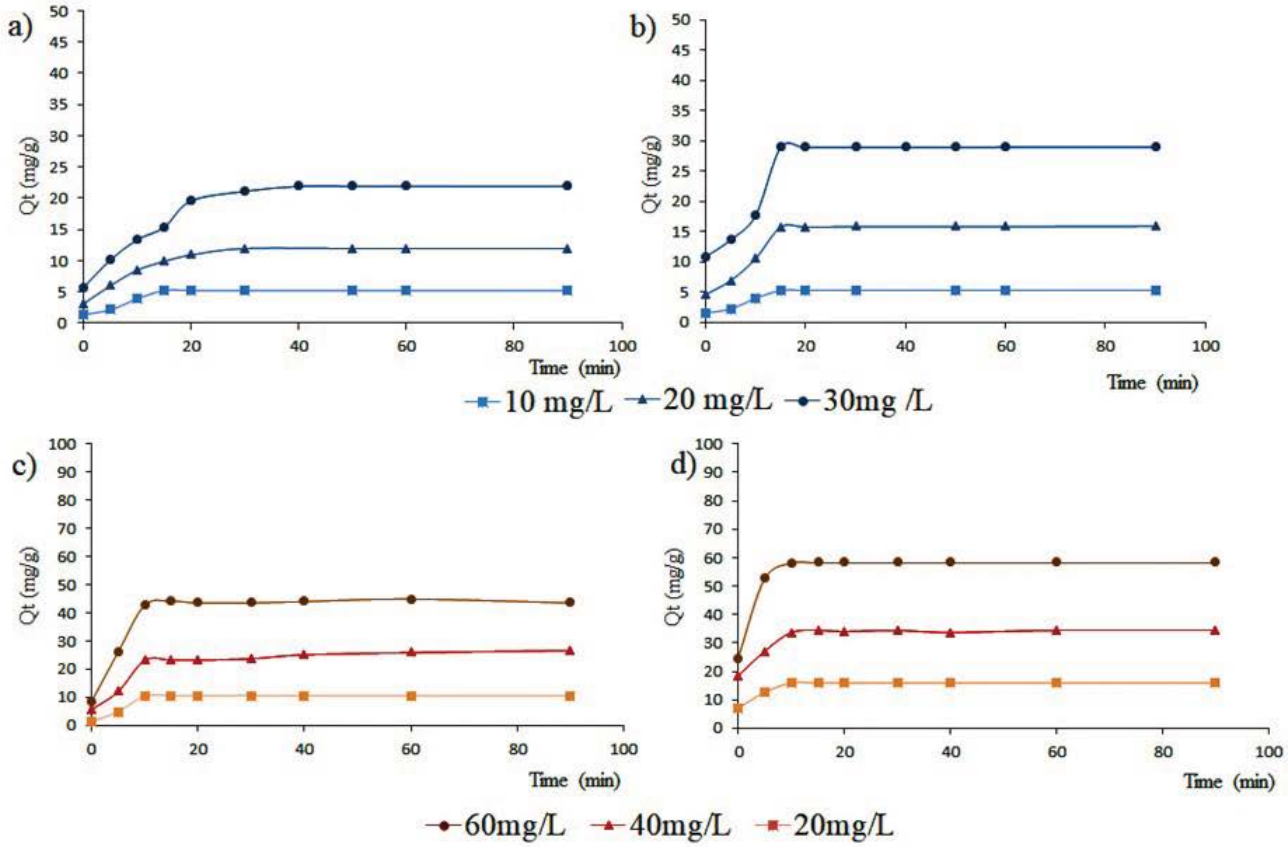

Fig. 5. Initial concentration effect on the adsorption of dyes onto ND and DAA: (a) adsorption of Methylene blue on ND, (b) adsorption of Methylene blue on DAA, (c) adsorption of Congo red on ND and (d) adsorption of Congo red on DAA.

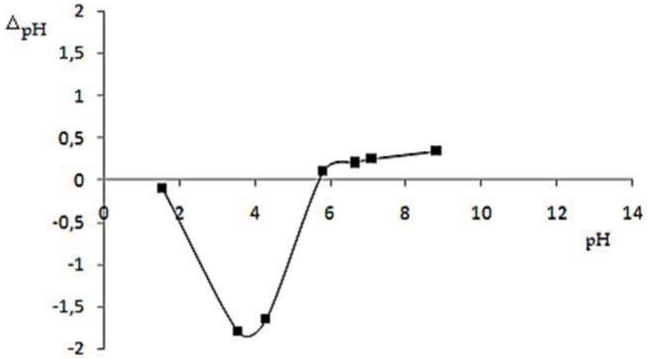

Fig. 6. Determination of pH_{pzc} of diatomite.

asymmetric vibration of Si–O–Si [45]. The presence of clays impurities in diatomite can be confirmed by the peak at 790 cm^{-1} [46]. The same results have been observed in previous studies, the analysis of a commercial diatomite showed that the main peaks of this rock are at 3,370; 1,471; 1,100; 800 and 468 cm^{-1} [47]. In addition, Du et al. [48] confirmed the presence of these peaks at 3,430; 1,633; 468; 1,098; 798 and 532 cm^{-1}. Thus, the presence of specific peaks in the spectrum of our treated diatomite proves its good quality.

In both spectra, we can notice a large band at 3,495 cm^{-1} corresponds to the stretching O–H groups. Simple peaks around 3,000 cm^{-1} can be attributed to aromatic C–H while those at 2,800 cm^{-1} correspond to aliphatic C–H. The strong asymmetric C–O–O stretching vibration bands confirmed at 1,650 and 1,388 cm^{-1} is caused by the presence of the alginate molecule [49]. By adding the activated carbon, the intensity of the peaks was reduced. In addition, we cannot exactly identify the two peaks at 1,650 and 1,388 cm^{-1} because they are warned of alginate molecules as well as activated carbon [50]. The two vibrations around 1,023 and around 460 cm^{-1} correspond to the asymmetric vibration of (Si–O–Si).

4.2. Effects operational parameter on MB and CR adsorption

4.2.1. Initial concentration effect

Despite the sufficient vacant active sites, the adsorption capacity at low concentration was low. This observation is in relation to the few numbers of molecules attaching with the adsorbent. The maximum percentage of elimination of MB by ND is 73.15% (19.95 mg/g) at pH 6, at a stirring rate of 150 rpm, and 0.1 g of absorbent at 25°C for a concentration of 30 mg/L. While this percentage is 96.72% (30.02 mg/L) using modified diatomite under the same conditions. In other hand, and for CR, the percentage increases from 72.63% (44.93 mg/L) up to 97.21% (85.32 mg/L), for a concentration of 60 mg/L, at pH 3, stirring speed 150 rpm and at 25°C. Our observations regarding the increase in adsorption capacity with the initial concentration correlate with other

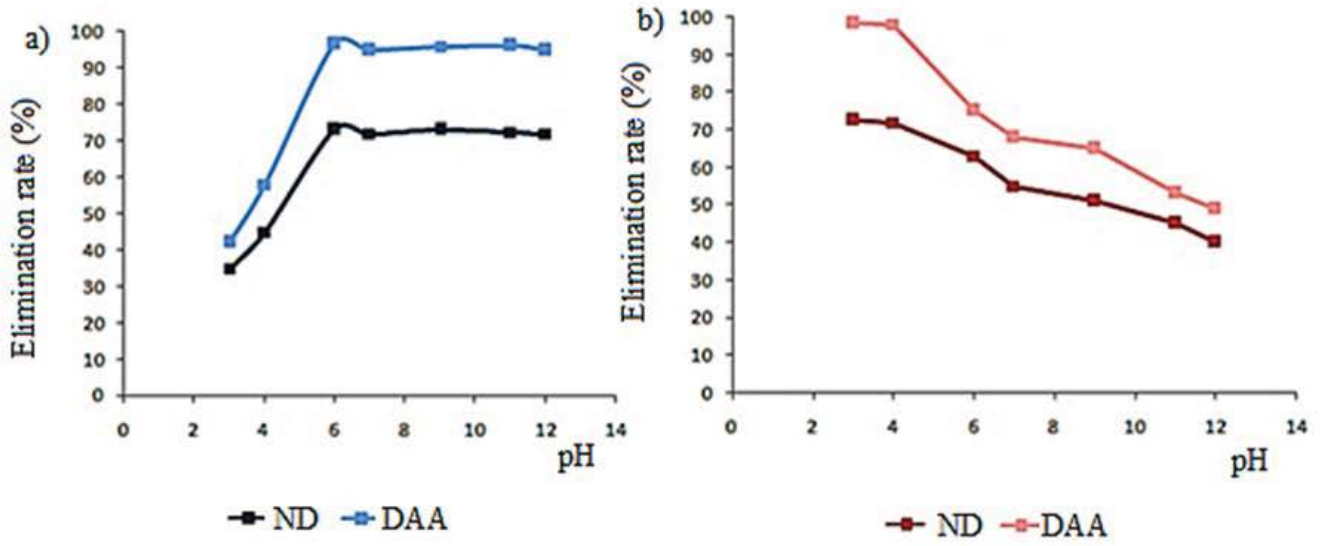

Fig. 7. Effect of pH on the adsorption dyes on ND and DAA: (a) effect of pH on the adsorption of Methylene blue on ND and DAA and (b) effect of pH on the adsorption of Congo red on ND and DAA.

Table 2
Parameters of pseudo-first-order and pseudo-second-order

Adsorbants	Kinetic models	Parameters	Methylene blue			Congo red		
			30 mg/L	20 mg/L	10 mg/L	20 mg/L	40 mg/L	60 mg/L
ND	Pseudo-first-order	$Q_{e,cal}$ (mg/g)	10.74	4.06	0.39	1.49	5.52	5.74
		$Q_{e,exp}$ (mg/g)	22	12.03	5.18	10.51	25.9	45
		k_1 (min^{-1})	0.034	0.039	0.029	0.019	0.013	0.016
		R^2	0.802	0.736	0.451	0.325	0.196	0.368
	Pseudo-second-order	$Q_{e,cal}$ (mg/g)	23.81	12.65	5.49	10.75	27.78	45.45
		$Q_{e,exp}$ (mg/g)	22	12.03	5.18	10.51	25.9	45
		k_2 (g/mg·min)	0.009	0.027	0.66	0.067	0.012	0.028
		R^2	0.992	0.996	0.987	0.995	0.996	0.998
DAA	Pseudo-first-order	$Q_{e,cal}$ (mg/g)	3.622	3.88	0.64	0.76	2.19	2.25
		$Q_{e,exp}$ (mg/g)	29.2	15.98	6.56	15.9	34.5	58.5
		k_1 (min^{-1})	0.021	0.026	0.029	0.015	0.016	0.026
		R^2	0.456	0.653	0.548	0.348	0.419	0.592
	Pseudo-second-order	$Q_{e,cal}$ (mg/g)	30.3	16.67	6.76	16.13	34.48	58.82
		$Q_{e,exp}$ (mg/g)	29.2	15.98	6.56	–	–	–
		k_2 (g/mg·min)	0.013	0.022	0.088	0.19	0.07	0.145
		R^2	0.993	0.993	0.997	0.999	0.999	1

Table 3
Parameters of Langmuir and Freundlich of dyes adsorption

		Parameters of Freundlich			Parameters of Langmuir		
		K_f	$1/n$	R^2	Q_m (mg/g)	K_l (L/mg)	R^2
ND	Methylene blue	5.8	0.941	0.932	83.33	1.004	0.972
	Congo red	2.4	0.983	0.897	333.33	0.006	0.966
DAA	Methylene blue	3.13	0.906	0.979	100	0.032	0.989
	Congo red	8.27	0.73	0.997	700	0.011	0.999

Table 4
Thermodynamic parameters

Adsorbants	Dyes	T (°C)	$\Delta H°$ (kJ/mol)	$\Delta S°$ (kJ/mol)	$\Delta G°$ (kJ/mol)
ND	Methylene blue	25	–46.52	–0.16	–0.31
		35			–1.61
		45			2.78
	Congo red	25	–23.94	–0.073	–2.002
		35			–1.21
		45			–0.53
DAA	Methylene blue	25	–45.01	–0.078	–1.504
		35			–0.89
		45			0.077

Table 5
Comparison of the efficiency adsorption (%) of dyes on different adsorbent material based on diatomite

Adsorbent Material	Dyes	Adsorption Efficiency (%)	Refs
DAA	Methylene Blue	96.72	Present study
DAA	Congo Red	97.21	Present study
La@D-0.1	Methylene Blue	86.4	[52]
spent diatomite	Methylene Blue	95.5	[53]
DBPC@ZIF-67	Congo Red	95.53	[54]
Porous diatomite microspheres	Methylene Blue	95.6	[55]
chitosan/diatomite composite	Methyl Orange	88.37	[56]
Poly (ethylene diamine-trimesoyl chloride)-modified diatomite	Rhodamine B	80	[57]
Diatomite/Manganese silicate nanosheet composites	Malachite Green	93	[58]

research which confirms the increased rate of removal of MB and CR by bentonite/zeolite-NaP. This material was able to remove 94% of MB and 93% of CR after 720 min 5 mg/L [51]. The observation confirms that the modification of the DE by activated carbon increases the absorption capacity of the adsorbent. This increase is due to the specific characteristics of activated carbon such as its porosity.

In addition, the adsorption of other modified diatomite tested for the removal of dyes in previous studies is listed in Table 5. It is clear that DAA has a good adsorption capacity (96.72% and 97.21% for MB and CR, respectively) compared to the other adsorbents [52–58].

4.2.2. Effect of pH

Thus, in an acidic environment, an electrostatic attraction occurs between the positive charges of the two surfaces of the adsorbent and the molecules of Congo red, which leads to a high adsorption capacity. However, at pH greater than 5.4, the exuberance OH^- on the surface of diatomite involves a concurrence between OH^- and anionic adsorbate molecules, provoking a repulsive force between the negative charges of the de anionic dye and adsorbent surface charges, which reduce the efficiency of dye adsorption and the opposite for MB molecules [59,60]. Similar studies have been reported, Yu et al. [61], for example, showed that the best pH for the adsorption of MB by mesoporous silica nanoparticles prepared with DE was also at a basic pH. Bayramoglu and Arica [62] used native amine and carboxyl modified biomass for the adsorption of Congo red, thus, an acidic pH promotes adsorption capacity.

4.3. Adsorption kinetic model

The correlation coefficient (R_1) of the pseudo-first-order model is far from 1 and the values calculated $Q_{e,\text{cal}}$ and experimental $Q_{e,\text{exp}}$ are so far, this kinetic model is not valid. However, the linear line of the pseudo-second-order, we can confirm that the later can describe better the adsorption process which confirm that this kinetic model is valid [63].

4.4. Adsorption isotherm

According to the values of the regression coefficients (R^2) the absorption followed the Langmuir model (R^2 Langmuir > R^2 Freundlich. In addition, the values of n given by the Freundlich model ($1/n < 1$) confirm that the adsorption is favorable. The same results have been reported by Liu et al. [64] for the adsorption of these two dyes by nutshells.

4.5. Thermodynamic study

According to our results, the negatives values of $\Delta H°$ and $\Delta S°$ indicate that the adsorption phenomenon is physical, favorable and spontaneous process at 25°C and 35°C. However, the positive values of $\Delta G°$ for the adsorption of MB at 45°C confirm that the adsorption is not favorable and not spontaneous [65].

5. Conclusions

Novel composite of diatomite modified by activated carbon beads was successfully synthesized as a potential adsorbent for Methylene blue and Congo red dyes from aqueous solution. The characterization confirmed that diatomite has a porous structure and is very rich in SiO_2 which favor the adsorption process. In addition, the results confirmed that prepared beads contain numerous balls of all the composites which causes a heterogeneous and rough surface. Thus, the effects of experimental conditions such as adsorption kinetic and isotherm were studied in detail. The activated carbon significantly enhanced the adsorption capacity of diatomite. The results showed that the optimized values of pH and adsorbent dose were found to be 6 for Methylene blue and 3 for Congo red. In relation to the fitted models to the kinetic data, the pseudo-second-order can describe the adsorption. Moreover, the Langmuir model describes well the adsorption process of dyes. The thermodynamic studies indicated that the adsorption phenomenon is physical, favorable and spontaneous at 25°C and 35°C according to the negative values of $\Delta H°$ and $\Delta S°$. However, the positive values of $\Delta G°$ for the adsorption of MB at 45°C confirm that the adsorption is not favorable and not spontaneous.

Considering the obtained results, it can be concluded that the combination of diatomite-alginate-activated carbon is an excellent adsorbent for dyes removal.

References

[1] S. Parvin, B.K. Biswas, Md A. Rahman, Md H. Rahman, Md S. Anik, Md R. Uddin, Study on adsorption of Congo red onto chemically modified egg shell membrane, Chemosphere, 236 (2019) 124326, doi: 10.1016/j.chemosphere.2019.07.057.

[2] A.B. Daphedar, S. Kakkalameli, B. Faniband, M. Bilal, R.N. Bhargava, L.F.R. Ferreira, A. Rahdar, D.M. Gurumurthy, S.I. Mulla, Decolorization of various dyes by microorganisms and green-synthesized nanoparticles: current and future perspective, Environ. Sci. Pollut. Res. Int., (2022) 1–16, doi: 10.1007/s11356-022-21196-9.

[3] S. Mishra, J.K. Nayak, A. Maiti, Bacteria-mediated biodegradation of reactive azo dyes coupled with bio-energy generation from model wastewater, Clean Technol. Environ. Policy, 22 (2020) 651–667.

[4] M. Shabir, M. Yasin, M. Hussain, I. Shafiq, P. Akhter, A.-S. Nizami, B.-H. Jeon, Y.-K. Park, A review on recent advances in the treatment of dye-polluted wastewater, J. Ind. Eng. Chem., 112 (2022) 1–19.

[5] S. Benkhaya, S. M'rabet, A. El Harfi, A review on classifications, recent synthesis and applications of textile dyes, Inorg. Chem. Commun., 115 (2020) 107891, doi: 10.1016/j.inoche.2020.107891.

[6] S. Baruah, A. Devi, K.G. Bhattacharyya, A. Sarma, Developing a biosorbent from *Aegle Marmelos* leaves for removal of Methylene blue from water, Int. J. Environ. Sci. Technol., 14 (2012) 341–352.

[7] P.O. Oladoye, T.O. Ajiboye, E.O. Omotola, O.J. Oyewola, Methylene blue dye: toxicity and potential elimination technology from wastewater, Results Eng., 16 (2022) 100678, doi: 10.1016/j.rineng.2022.100678.

[8] W.-T. Tsai, K.-J. Hsien, H.-C. Hsu, Adsorption of organic compounds from aqueous solution onto the synthesized zeolite, J. Hazard. Mater., 166 (2009) 635–641.

[9] R. Saha, M. Mukhopadhyay, Elucidation of the decolorization of Congo red by *Trametes versicolor* laccase in presence of ABTS through cyclic voltammetry, Enzyme Microb. Technol., 135 (2020) 109507, doi: 10.1016/j.enzmictec.2019.109507.

[10] N. Asses, L. Ayed, N. Hkiri, M. Hamdi, Congo red decolorization and detoxification by *Aspergillus niger*: removal mechanisms and dye degradation pathway, Biomed Res. Int., 2018 (2018) 3049686, doi: 10.1155/2018/3049686.

[11] S.A. Bhat, F. Zafar, A.H. Mondal, A.U. Mirza, Q.M.R. Haq, N. Nishat, Efficient removal of Congo red dye from aqueous solution by adsorbent films of polyvinyl alcohol/melamine-formaldehyde composite and bactericidal effects, J. Cleaner Prod., 255 (2020) 120062, doi: 10.1016/j.jclepro.2020.120062.

[12] D. Sakhi, Y. Rakhila, A. Elmchaouri, M. Abouri, S. Souabi, A. Jada, Optimization of Coagulation Flocculation Process for the Removal of Heavy Metals from Real Textile Wastewater, M. Ezziyyani, Ed., Advanced Intelligent Systems for Sustainable Development (AI2SD'2018), AI2SD 2018, Advances in Intelligent Systems and Computing, Vol. 913, Springer, Cham, 2019. https://doi.org/10.1007/978-3-030-11881-5_22

[13] H.R. Shamsollahi, M. Alimohammadi, S. Momeni, K. Naddafi, R. Nabizadeh, F.C. Khorasgani, M. Masinaei, M. Yousefi, Assessment of the health risk induced by accumulated heavy metals from anaerobic digestion of biological sludge of the lettuce, Biol. Trace Elem. Res., 188 (2019) 514–520.

[14] R.D. Tyagi, D. Couillard, F. Tran, Heavy metals removal from anaerobically digested sludge by chemical and microbiological methods, Environ. Pollut., 50 (1988) 295–316.

[15] C.V.T. Rigueto, M.T. Nazari, M. Rosseto, L.A. Massuda, I. Alessandretti, J.S. Piccin, A. Dettmer, Emerging contaminants adsorption by beads from chromium(III) tanned leather waste recovered gelatin, J. Mol. Liq., 330 (2021) 115638, doi: 10.1016/j.molliq.2021.115638.

[16] L. Kong, A. Enders, T.S. Rahman, P.A. Dowben, Molecular adsorption on graphene, J. Phys. Condens. Matter, 26 (2014) 443001, doi: 10.1088/0953-8984/26/44/443001.

[17] A.K. Ghoshal, S.D. Manjare, Selection of appropriate adsorption technique for recovery of VOCs: an analysis, J. Loss Prev. Process Ind., 15 (2002) 413–421.

[18] M. Hasan, A.N. Banerjee, M. Lee, Enhanced thermo-optical performance and high BET surface area of graphene@PVC nanocomposite fibers prepared by simple facile deposition technique: N_2 adsorption study, J. Ind. Eng. Chem., 21 (2015) 828–834.

[19] C. Yang, Y. Wang, H. Fan, G. de Falco, S. Yang, J. Shangguan, T.J. Bandosz, Bifunctional ZnO-MgO/activated carbon adsorbents boost H_2S room temperature adsorption and catalytic oxidation, Appl. Catal., B, 266 (2020) 118674, doi: 10.1016/j.apcatb.2020.118674.

[20] N. Tahari, H. Nefzi, A. Labidi, S. Ayadi, M. Abderrabba, J. Labidi, Removal of Dyes and Heavy Metals with Clays and Diatomite, Inamuddin, M.I. Ahamed, E. Lichtfouse, Eds., Water Pollution and Remediation: Heavy Metals, Environmental Chemistry for a Sustainable World, Vol. 53, Springer, Cham, 2021. https://doi.org/10.1007/978-3-030-52421-0_16

[21] D. Zuluaga-Astudillo, J.C. Ruge, J. Camacho-Tauta, O. Reyes-Ortiz, B. Caicedo-Hormaza, Diatomaceous soils and advances in geotechnical engineering—Part I, Appl. Sci., 13 (2023) 549, doi: 10.3390/app13010549.

[22] M. Rigaux, E. Haubruge, P.G. Fields, Mechanisms for tolerance to diatomaceous earth between strains of *Tribolium castaneum*, Entomol. Exp. Appl., 101 (2001) 33–39.

[23] T. Benkacem, B. Hamdi, A. Chamayou, H. Balard, R. Calvet, Physicochemical characterization of a diatomaceous upon an acid treatment: a focus on surface properties by inverse gas chromatography, Powder Technol., 294 (2016) 498–507.

[24] T. Ma, Y. Wu, N. Liu, Y. Wu, Hydrolyzed polyacrylamide modified diatomite waste as a novel adsorbent for organic dye removal: adsorption performance and mechanism studies, Polyhedron, 175 (2020) 114227, doi: 10.1016/j.poly.2019.114227.

[25] S. Yan, W. Huo, J. Yang, X. Zhang, Q. Wang, L. Wang, Y. Pan, Y. Huang, Green synthesis and influence of calcined temperature on the formation of novel porous diatomite microspheres for efficient adsorption of dyes, Powder Technol., 329 (2018) 260–269.

[26] R. Gao, L. Wang, E. Wang, J. He, J. Huang, X. Hou, Adsorption kinetics and thermodynamics of hydroquinone with aid of diatomite-modified wood ceramics, Ceram. Int., 49 (2023) 17109–17115.

[27] M. Rinaudo, Main properties and current applications of some polysaccharides as biomaterials, Polym. Int., 57 (2008) 397–430.
[28] A. Łętocha, M. Miastkowska, E. Sikora, Preparation and characteristics of alginate microparticles for food, pharmaceutical and cosmetic applications, Polymers, 14 (2022) 3834, doi: 10.3390/polym14183834.
[29] A. Kumar, T. Das, R.S. Thakur, Z. Fatima, S. Prasad, N.G. Ansari, D.K. Patel, Synthesis of biomass-derived activated carbons and their immobilization on alginate gels for the simultaneous removal of Cr(VI), Cd(II), Pb(II), As(III), and Hg(II) from water, ACS Omega, 7 (2022) 41997–42011.
[30] P. Agulhon, M. Robitzer, J.-P. Habas, F> Quignard, Influence of both cation and alginate nature on the rheological behavior of transition metal alginate gels, Carbohydr. Polym., 112 (2014) 525–531.
[31] S. Lilhare, S.B. Mathew, A.K. Singh, S.A.C. Carabineiro, *Aloe vera* functionalized magnetic nanoparticles entrapped Ca alginate beads as novel adsorbents for Cu(II) removal from aqueous solutions, Nanomaterials, 12 (2022) 2947, doi: 10.3390/nano12172947.
[32] L.K. Njaramba, S. Kim, Y. Kim, B. Cha, N. Kim, Y. Yoon, C.M. Park, Remarkable adsorption for hazardous organic and inorganic contaminants by multifunctional amorphous core–shell structures of metal–organic framework-alginate composites, Chem. Eng. J., 431 (2022) 133415, doi: 10.1016/j.cej.2021.133415.
[33] B.H.D. Son, V.Q. Mai, D.X. Du, N.H. Phong, D.Q. Khieu, A study on astrazon black AFDL dye adsorption onto Vietnamese diatomite, J. Chem., 2016 (2016) 8685437, doi: 10.1155/2016/8685437.
[34] B. Stoean, L. Gaina, C. Cristea, R. Silaghi-Dumitrescu, A.M.V. Branzanic, M. Focsan, E. Fischer-Fodor, B. Tigu, C. Moldovan, A.D. Cecan, P. Achimas-Cadariu, S. Astilean, L. Silaghi-Dumitrescu, New Methylene blue analogues with N-piperidinyl-carbinol units: synthesis, optical properties and *in vitro* internalization in human ovarian cancer cells, Dyes Pigm., 205 (2022) 110460, doi: 10.1016/j.dyepig.2022.110460.
[35] M. Najafi, T.R. Bastami, N. Binesh, A. Ayati, S. Emamverdi, Sono-sorption versus adsorption for the removal of Congo red from aqueous solution using NiFeLDH/Au nanocomposite: kinetics, thermodynamics, isotherm studies, and optimization of process parameters, J. Ind. Eng. Chem., 116 (2022) 489–503.
[36] S.Y. Lagergren, Zur Theorie der sogenannten Adsorption gelöster Stoffe, K. Sven. Vetenskapsakad. Handl., 24 (1988) 1–39.
[37] Y.S. Ho, G. McKay, Pseudo-second-order model for sorption processes, Process Biochem., 34 (1999) 451–465
[38] H.M.F. Freundlich, Over the adsorption in solution, J. Phys. Chem., 57 (1906) 385–471.
[39] I.J. Langmuir, The constitution and fundamental properties of solids and liquids. Part I solids, J. Am. Chem. Soc., 38 (1916) 2221–2295.
[40] E. Kır, H. Oruc, I. Kır, T. Sardohan-Koseoglu, Removal of fluoride from aqueous solution by natural and acid-activated diatomite and ignimbrite materials, Desal. Water Treat., 57 (2016) 21944–21956.
[41] A. Benhouria, Md A. Islam, H. Zaghouane-Boudiaf, M. Boutahala, B.H. Hameed, Calcium alginate–bentonite–activated carbon composite beads as highly effective adsorbent for Methylene blue, Chem. Eng. J., 270 (2015) 621–630.
[42] O.O. Ikusika, C.T. Mpendulo, T.J. Zindove, A.I. Okoh, Fossil shell flour in livestock production: a review, Animals, 9 (2019) 70, doi: 10.3390/ani9030070.
[43] H. Nefzi, M. Abderrabba, S. Ayadi, J. Labidi, Formation of palygorskite clay from treated diatomite and its application for the removal of heavy metals from aqueous solution, Water, 10 (2018) 1257, doi: 10.3390/w10091257.
[44] H. Nefzi, A.M. Salaberria, M. Abderrabbaa, S. Ayadi, J. Labidi, Cellulose modified diatomite for toluene removal from aqueous solution, Desal. Water Treat., 150 (2019) 228–236.
[45] J. Mohammed, N.S. Nasri, M.A.A. Zaini, U.D. Hamza, F.N. Ani, Adsorption of benzene and toluene onto KOH activated coconut shell based carbon treated with NH_3, Int. Biodeterior. Biodegrad., 102 (2015) 245–255.
[46] I.I. Ilia, M. Stamatakis, T.S. Perraki, Mineralogy and technical properties of clayey diatomites from north and central Greece, Cent. Eur. J. Geosci., 1 (2009) 393–403.
[47] L. Jiang, L. Liu, S. Xiao, J. Chen, Preparation of a novel manganese oxide-modified diatomite and its aniline removal mechanism from solution, Chem. Eng. J., 284 (2016) 609–619.
[48] Y. Du, X. Wang, J. Wu, C. Qi, Y. Li, Adsorption and photoreduction of Cr(VI) via diatomite modified by Nb_2O_5 nanorods, Particuology., 40 (2018) 123–130.
[49] R. Pereira, A. Tojeira, D.C. Vaz, A. Mendes, P. Bártolo, Preparation and characterization of films based on alginate and *Aloe vera*, Int. J. Polym. Anal. Charact., 16 (2011) 449–464.
[50] F.W. Shaarani, B.H. Hameed, Ammonia-modified activated carbon for the adsorption of 2,4-dichlorophenol, Chem. Eng. J., 169 (2011) 180–185.
[51] M. Shaban, M.R. Abukhadra, M.G. Shahien, S.S. Ibrahim, Novel bentonite/zeolite-NaP composite efficiently removes Methylene blue and Congo red dyes, Environ. Chem. Lett., 16 (2018) 275–280.
[52] N. Dai, L. Feng, L. Zhao, D. Song, X.J. Dai, X.Y. Liu, Y.X. Zhang, A high-performance adsorbent of 2D laponite *in-situ* coated on 3D diatomite for advanced adsorption of cationic dye, Sci. China Technol. Sci., 65 (2022) 2304–2316.
[53] X. Gong, W. Tian, L. Wang, J. Bai, K. Qiao, J. Zhao, Biological regeneration of brewery spent diatomite and its reuse in basic dye and chromium(III) ions removal, Process Saf. Environ. Prot., 128 (2019) 353–361.
[54] Y. Feng, Z. Zhuang, Q. Zeng, D. Liu, Porous ceramic-based metal–organic framework DBPC@ZIF-67 for the efficient removal of Congo red from an aqueous solution, Cryst. Growth Des., 21 (2011) 5172–5182.
[55] S. Yan, W. Huo, J. Yang, X. Zhang, Q. Wang, L. Wang, Y. Pan, Y. Huang, Green synthesis and influence of calcined temperature on the formation of novel porous diatomite microspheres for efficient adsorption of dyes, Powder Technol., 329 (2018) 260–269.
[56] P. Zhao, R. Zhang, J. Wang, Adsorption of methyl orange from aqueous solution using chitosan/diatomite composite, Water Sci. Technol., 75 (2017) 1633–1642.
[57] T.A. Saleh, M. Tuzen, A. Sarı, Evaluation of poly(ethylene diamine-trimesoyl chloride)-modified diatomite as efficient adsorbent for removal of rhodamine B from wastewater samples, Environ. Sci. Pollut. Res., 28 (2021) 55655–55666.
[58] D.B. Jiang, Y. Yuan, D. Zhao, K. Tao, X. Xu, Y.X. Zhang, Facile synthesis of three-dimensional diatomite/manganese silicate nanosheet composites for enhanced Fenton-like catalytic degradation of malachite green dye, J. Nanopart. Res., 20 (2018) 1–10, doi: 10.1007/s11051-018-4226-2.
[59] S. Pal, A.S. Patra, S. Ghorai, A.K. Sarkar, V. Mahato, S. Sarkar, R.P. Singh, Efficient and rapid adsorption characteristics of templating modified guar gum and silica nanocomposite toward removal of toxic reactive blue and Congo red dyes, Bioresour. Technol., 191 (2015) 291–299.
[60] S. Ghorai, A.K. Sarkar, A.B. Panda, S. Pal, Effective removal of Congo red dye from aqueous solution using modified xanthan gum/silica hybrid nanocomposite as adsorbent, Bioresour. Technol., 144 (2013) 485–491.
[61] Z.-H. Yu, S.-R. Zhai, H. Guo, T.-M. Lv, Y. Song, F. Zhang, H.-C. Ma, Removal of Methylene blue over low-cost mesoporous silica nanoparticles prepared with naturally occurring diatomite, J. Sol-Gel Sci. Technol., 88 (2018) 541–550.
[62] G. Bayramoglu, M.Y. Arica, Adsorption of Congo red dye by native amine and carboxyl modified biomass of *Funalia trogii*: isotherms, kinetics and thermodynamics mechanisms, Korean J. Chem. Eng., 35 (2018) 1303–1311.
[63] V. Vimonses, S. Lei, B. Jin, C.W.K. Chow, C. Saint, Kinetic study and equilibrium isotherm analysis of Congo red adsorption by clay materials, Chem. Eng. J., 148 (2009) 354–364.
[64] M. Liu, X. Li, Y. Du, R. Han, Adsorption of methyl blue from solution using walnut shell and reuse in a secondary adsorption for Congo red, Bioresour. Technol. Rep., 5 (2019) 238–242.
[65] K.G. Bhattacharyya, A. Sharma, Kinetics and thermodynamics of Methylene blue adsorption on neem (*Azadirachta indica*) leaf powder, Dyes Pigm., 65 (2005) 51–59.